

Article

Comparative Studies of Blue-Emitting Zinc Selenide Nanocrystals Doped with Ag, Cu, and Mg towards Medical Applications

Van Khiem Nguyen^{1,2,3}, Duy Khanh Pham^{1,4}, Ngoc Quyen Tran^{1,4}, Le Hang Dang^{1,4}, Ngoc Hoa Nguyen⁵, Thanh Viet Nguyen⁶, Thi Hiep Nguyen^{2,3} and Thi Bich Luong^{1,3,*}

¹ Institute of Applied Materials Science, Viet Nam Academy of Science and Technology, Ha Noi 100000, Vietnam; nvkhiem@iams.vast.vn (V.K.N.); duykhanhsn@iams.vast.vn (D.K.P.); tnquyen@iams.vast.vn (N.Q.T.); dtlhang@iams.vast.vn (L.H.D.)

² School of Biomedical Engineering, International University, Ho Chi Minh City 700000, Vietnam; nthiep@hcmiu.edu.vn

³ Vietnam National University, Ho Chi Minh City 700000, Vietnam

⁴ Graduate University of Science and Technology, Vietnam Academy of Science and Technology, Ha Noi 100000, Vietnam

⁵ Faculty of Chemical Engineering, HCMC University of Food Industry, Ho Chi Minh City 700000, Vietnam; hoann@hufi.edu.vn

⁶ Institute of Technology Application and Sustainable Development, Nguyen Tat Thanh University, Ho Chi Minh City 700000, Vietnam; ntviet@ntt.edu.vn

* Correspondence: luongthibich@iams.vast.vn; Tel.: +84-0395-450-266



Citation: Nguyen, V.K.; Pham, D.K.; Tran, N.Q.; Dang, L.H.; Nguyen, N.H.; Nguyen, T.V.; Nguyen, T.H.; Luong, T.B. Comparative Studies of Blue-Emitting Zinc Selenide Nanocrystals Doped with Ag, Cu, and Mg towards Medical Applications. *Crystals* **2022**, *12*, 625. <https://doi.org/10.3390/cryst12050625>

Academic Editors: Mohammed Rafi Shaik, Syed Farooq Adil and Mujeeb Khan

Received: 15 March 2022

Accepted: 23 April 2022

Published: 27 April 2022

Publisher's Note: MDPI stays neutral with regard to jurisdictional claims in published maps and institutional affiliations.



Copyright: © 2022 by the authors. Licensee MDPI, Basel, Switzerland. This article is an open access article distributed under the terms and conditions of the Creative Commons Attribution (CC BY) license (<https://creativecommons.org/licenses/by/4.0/>).

Abstract: Blue-emitting Ag⁽⁺⁾-, Cu⁽²⁺⁾-, and Mg⁽²⁺⁾-doped ZnSe nanoparticles (NPs) were successfully synthesized at 80 °C by the precipitation method by using mercaptopropionic acid (MPA) as a stabilizer. UV-visible and photoluminescence (PL) studies were applied to investigate their physicochemical properties. Their structural properties were confirmed by X-ray diffraction (XRD), Fourier transform infrared (FT-IR) and transmission electron microscopy (TEM). The size of the ZnSe: X-capped MPA showed a strong relationship with dopant metals. The diameters of the Mg-doped ZnSe and the Cu-doped ZnSe were 22–24 nm, while the Ag-doped ZnSe was halved, at about 13 nm. The photoluminescence was within a wavelength range of 400–550 nm. In addition, the PL intensities, as well as the photoluminescence quantum yields, were in the order of the decreasing ionic radii of the dopant metals (ZnSe:Ag < ZnSe:Mg < ZnSe:Cu). Furthermore, through the interaction with lysine, the PL intensity of the ZnSe:X was changed. Interestingly, the capacity of the ZnSe:Mg for lysine was significantly higher than that of other dopant metals. Moreover, the toxicity of the ZnSe:Mg was relatively insignificant toward the hMSCs (about 80% cell viability at 320 ppm), compared to the transition-metal dopant. Therefore, the ZnSe:Mg material could have great potential for bioapplications.

Keywords: luminescent nanoparticles; green synthesis; blue emission

1. Introduction

With remarkable characteristics, such as unique chemical and physical properties, large specific surface areas, and high bioactivity, semiconducting nanoparticles have become good candidates to replace traditional organic antimicrobial agents, which are extremely irritant and toxic. Currently, fluorescent dyes are being widely replaced by quantum dots (QDs) as effective alternatives or complementary tools in advanced biosensors [1], cell imaging [2], and in vivo animal tracking [3], which is due to their photostability, high photoluminescence, narrow emissions, and broad UV excitation. Since fluorescent detection is necessary for both the studies of complex microbial populations and the identification of bacteria, the construction of probe-conjugated QDs for single-bacterium imaging is one of

the research areas with the most potential in the biological applications of QDs. Therefore, the tunability in the optics of QDs is greatly required in this field.

Nanocrystalline semiconductors that belong to the II–VI groups have attracted much attention because of the tunability of their band gaps [4–7] and their potential biomedical applications [8]. Among them, zinc selenide (ZnSe), which is a well-known n-type direct bandgap semiconductor [9–12] with highly intense luminescence properties and a wide band gap (bulk bandgap 2.8 eV), has been widely applied in light-emitting diodes, photodetectors, full color displays [13–16], and sensors [17–19]. In addition, ZnSe nanoparticles (NPs) demonstrate excellent biocompatibility, and they are also nontoxic to biological organisms [5]. However, the emission of ZnSe is in the violet region, which hinders its application in medical devices.

Various studies suggest that the optical performance of ZnSe NPs could be tunable by changing the type and the amount of the dopant [20–24]. Typically, when dopants are incorporated into ZnSe NPs, the charge extraction is reconstructed, and, consequently, the band structures are tuned. Promising dopants are mostly transition metals, which have some empty d-orbitals that result in the formation of the new charge transfer, and that then reduces the self-absorption of the NPs [22,23].

In terms of biomedical application, the selection of transition metals as the dopant is very important. The degree of nontoxicity plays a critical point in the selection. Among the common dopants, copper, magnesium, and silver could be considered as the promising candidates. Silver possesses many advantages, such as good antibacterial ability, excellent biocompatibility, and satisfactory stability [25]. Silver can have an antibacterial effect when it is used in a small percentage, but it can be toxic in higher amounts [26]. Silver nanoparticles have been studied for their accumulation in an *Escherichia coli* (*E. coli*) membrane to effectively induce antibacterial effects [27]. Moreover, the use of silver for adjusting the emission band of ZnSe has been investigated. For example, silver-doped ZnSe nanowires were investigated in the range of 10 to 300 K, which produced a blue-light emission [28]. The incorporation of Ag into ZnSe exhibited a blue emission at a wavelength range from 504 to 585 nm, which suggests a wide range of applications in optical coding, white light-emitting diodes (LEDs), and bioimaging [29]. Moreover, the stability of ZnSe is improved following the addition of silver metal [30]. Therefore, the tunable electrical and optical silver (Ag)-doped ZnSe thin films could be applied to make transistors and to work as the buffer layer in solar cells [31]. Similar to silver, copper has been proven to have antibacterial properties that particularly target multidrug-resistant bacteria. The abundance and the low cost of copper make it a better choice to work with, compared to silver. Moreover, by adding copper into ZnSe NPs, the excited stage of ZnSe NPs is overlapped with the emissive centers of the dopant, which induces the tunable emission characteristics [28]. The introduction of Cu into ZnSe NC (Cu:ZnSe d-dots) caused the redshift of the emission from 465 to 495 nm [28]. The two dopants, Mg and Cu, were introduced into the host material in a two-step process by using polyvinyl alcohol (PVA), thioglycolic acid (TGA), and L-glutathione (GSH) as the capping agents, which induced the emission in the visible spectrum range [32–38]. Together with d-metal as the dopant, p-type doping, such as with magnesium, provides an interesting result. Mg²⁺-doped ZnSe nanoparticles were synthesized by the simple wet chemical method by using N-methylaniline (NMA), which showed a tunable optoelectronic and potential use in solution-processable devices [39]. Previous studies have synthesized Mg- or Cu-doped CdS/ZnSe (core/shell) and Mg- or Cu-doped CdS, which are cubic, quartzite, and blue emitting, through direct chemical solution routes in organic solvent [40].

In this study, we report a green synthesis in the water of low-toxic ZnSe:X nanoparticles, with the dopant (X) being silver, copper, or magnesium, to create the visible blue phosphorescence at 440–475 nm. The ZnSe:X NPs were synthesized by using mercaptopropionic acid (MPA) as a stabilizer at 80–100 °C. In this work, the effect of the dopant types on the optical crystal structure and the morphological properties were inclusive. Moreover, the difference in the fluorescent signal of the ZnSe:X NPs after adding lysine was investigated

in order to examine the selective activity of the dopants on a biological agent. Furthermore, in order to verify the potential application in biomedical devices, the cytotoxicity assay using human mesenchymal stem cells (hMSCs) was performed. This study provides critical points in the selection of the dopant for the future application of ZnSe NPs.

2. Materials and Methods

2.1. Chemicals

Silver nitrate (AgNO_3), copper chloride (CuCl_2), magnesium chloride (Mg) (99.99%), zinc acetate ($\text{Zn}(\text{CH}_3\text{COO})_2 \cdot 2\text{H}_2\text{O}$) (99.99%), 2-propanol (HPLC grade), 3-Mercaptopropionic acid (MPA) (99+%), sodium borohydride (NaBH_4) (96%), and selenium powder (99.5%). All of the chemicals were purchased from Sigma-Aldrich, with high purification.

2.2. Preparation of ZnSe:X-Capped MPA Nanocrystals

The Zn^{2+} precursor solution was prepared in a three-neck flask, following the literature method, by the dissolution of 10 mL of zinc acetate 0.1 M in 90 mL of DI water, with 1.0 mL of X salt (X: silver nitrate, copper chloride, and magnesium chloride), and 40 mL of MPA 0.1 M, and then the pH of this system was adjusted to a pH = 6.5 by using NaOH 2 M with vigorous stirring. This was kept in N_2 gas for 30 min to degas, and during the whole reaction process, and the NaHSe solution was injected into the Zn^{2+} precursor solution at room temperature. The mixture was continuously stirred to 80–100 °C, which relates to the capping agent, and it was refluxed for 3 h for ZnSe:X (1%) crystal growth, and it was aged for 24 h with precipitation. The precipitate was washed several times and was dried at room temperature in order to produce a material that readily disperses in water.

2.3. Characterization

The physico-chemical properties were surveyed by using photoluminescence spectroscopy and Fourier transform infrared (FT-IR) spectroscopy. The photoluminescence quantum yield (PL QY) of the nanoparticles was also measured, according to the method that is described in Crosby and Demas [5,6]. A D/Maxrnt 2000 powder X-ray diffractometer with Cu $\text{K}\alpha$ radiation ($\lambda = 1.5418 \text{ \AA}$) was used to perform the X-ray diffraction measurements. A JEM 2100F transmission microscope with an acceleration voltage of 200 kV was used to capture the TEM.

2.4. Cytotoxic Test

Cell culture: Human mesenchymal stem cells (hMSCs) (passages: 4) were provided by Lonza Bioscience. Cells were cultured in Dulbecco's Modified Eagle Medium (DMEM)-F12, HyClone), and were supplied with 10% fetal bovine serum (FBS) (Sigma-Aldrich, St. Louis, MI, USA), 1.2 g/L sodium bicarbonate (Sigma-Aldrich), and 1% penicillin–streptomycin (P4333, Sigma-Aldrich) at 37 °C, 5% CO_2 , and 90% humidity.

Cytotoxicity test: The hMSCs were seeded in 96-well plates at a density of 2×10^5 cell/well. After 24 h, the medium was removed and was then replaced by the new cultured media, which contained various concentrations of ZnSe:X-capped MPA (0, 60, 120, 240, and 320 ppm). An amount of 0 ppm was distilled in water, and the background control was the hMSCs with cultured media only. The plates were incubated at 37 °C in a humidified incubator with 5% CO_2 for 48 h. Then, an SRB assay (ab235935, Abcam) was applied, following the instructions of the manufacturer. The cell viability was calculated with regard to the absorbance of the background control. Each sample was repeated independently three times. The live/dead assay based on dual staining with acridine orange (AO)/propidium iodide (PI) was also conducted. Briefly, the culture media in each well was discarded, and then the new media containing 10 μL of AO (50 $\mu\text{g}/\text{mL}$) and 5 μL of PI (1 mg/mL) was added. After 5 min of incubation in a CO_2 incubator, the PBS (1X, Gibco) was used to wash the dye before adding the freshly completed DMEM-F12 media. The result was observed under an Andor confocal microscope (using 525 nm and 650 nm filters).

3. Results and Discussion

3.1. Synthesis and Characterization of ZnSe:X NPs

Figure 1a,b show the luminescence of the prepared NPs capping with MPA in the aqueous phase. The ZnSe:Ag, ZnSe:Cu, and ZnSe:Mg NPs emitted in the range of 445 to 475 nm, and redshifted from the silver to the magnesium dopant. The PL intensities of the ZnSe:Ag, ZnSe:Mg, and ZnSe:Cu increased in accordance with the decreasing ionic radius of the dopant metal. In addition, the photoluminescence quantum yields were: ZnSe:Ag(1%)-MPA (26%); ZnSe:Mg(1%)-MPA (32%); and ZnSe:Cu(1%)-MPA (40%).

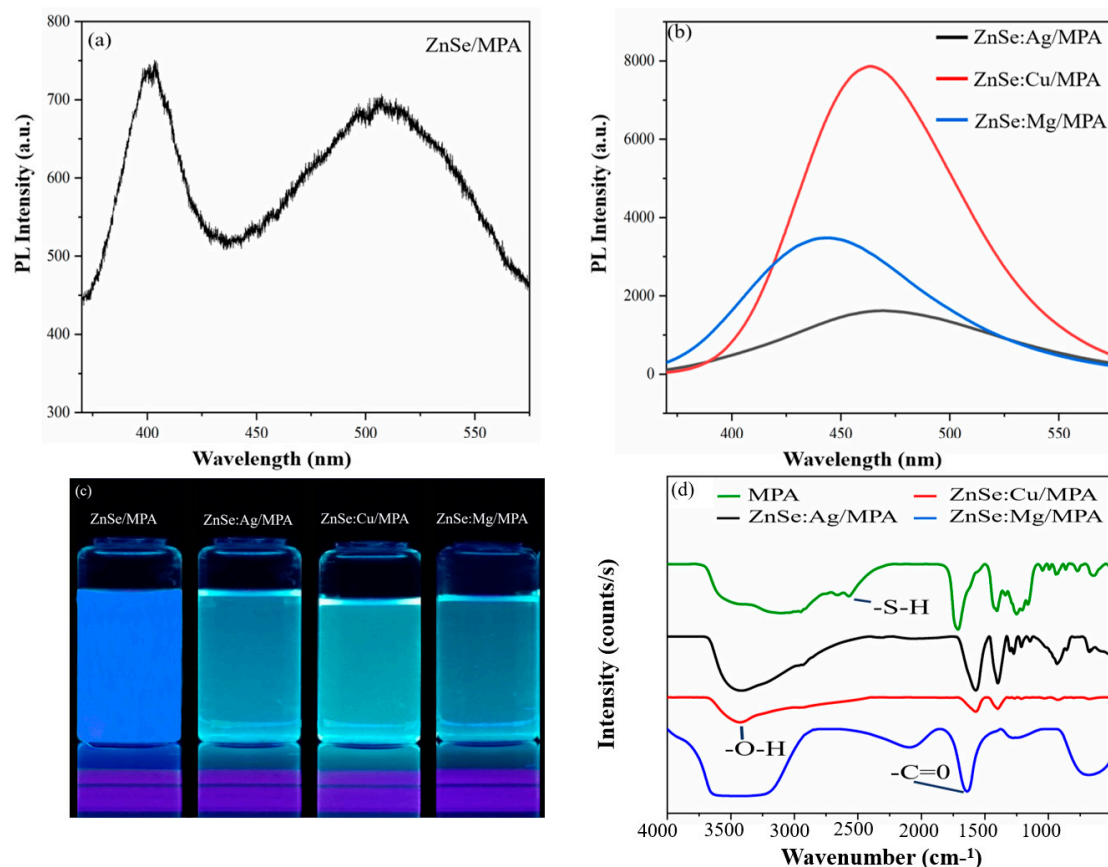


Figure 1. Photoluminescence spectra: (a) ZnSe-capped MPA; (b) ZnSe:Ag, ZnSe:Cu, and ZnSe:Mg; (c) a digital photograph of the UV-irradiated as-prepared solution; (d) FT-IR spectra of ZnSe:X (1%) nanoparticles under UV light ($\lambda_{exc} = 365$ nm).

By utilizing 365 nm as the excitation wavelength, the luminescence of ZnSe:Ag is at 445 nm, the luminescence of ZnSe:Cu is at 460 nm, and the luminescence of ZnSe:Mg is at 475 nm, which are similar to previous studies [32,33]. Actually, the ZnSe core NPs have two emission peaks: an obvious bandgap emission around 400 nm, and a defect emission around 500 nm [41]. The emission of the deep trap of the ZnSe is due to the suitable band gap (400 nm) [42,43], and the peak at a 500 nm wavelength is assigned either to the surface trap emission of the ZnSe stabilized by an MPA capping agent that is synthesized in the aqueous phase (see Figure 1a) [5], or to the trap state emission from the surface defects [44–48].

Compared to pure ZnSe NPs, the emission spectra of ZnSe:Ag contain only one broad peak at 445 nm. Silver ion activators provide the dominant nonradiative path via the deep levels for the excitation energy that are due to the effect of activator concentration quenching [49,50]. Ag:ZnSe and ZnSe NPs have different excitation processes, which suggests that the Ag impurities influenced the orbitals of the ZnSe. Obviously, photoinduced excitons

are more easily trapped by Ag impurities, which leads to the quenching of the band-gap emission of ZnSe NPs at 400 nm [51].

In the case of a copper doping agent, in comparison with ZnSe NPs, almost no bandgap emission is observed while the fluorescence emission peak of Cu^{2+} is exposed in the spectra, which makes the apparent PL change to blue green (Figure 1c). It is generally suggested that, under the level splitting of T_2 , electrons are formed at the conduction band of ZnSe between the valence band and the $3d^9$ ground state of Cu^{2+} . After the ZnSe matrix absorbs the energy, the electrons on the valence band jump to the conduction band, and then relax to the shallow donor energy level that is formed by the impurity ions (Cu^{2+}), and they then jump to the T_2 level of the Cu^{2+} to produce luminescence at around 460 nm [52–54]. There was no free Zn^{2+} in the Cu:ZnSe nanoparticle solution, as Zn^{2+} is in the form of ZnSe or Zn-MPA complexes. Cu ions also perform Cu-MPA complexes. Moreover, the -SH group of MPA acted as a reducing agent, which protected the aqueous Cu:ZnSe against oxidation by generating disulfides of MPA (di-MPA). The excess MPA efficiently prevented the oxidation of Cu:ZnSe, and increased the stability of the Cu:ZnSe d-dots [54–57]. Figure 1b also shows the photoluminescence spectrum of the Mg^{2+} -doped ZnSe NPs. It is the near-band-edge emission peak, which was observed at 475 nm, which is similar to a previous study [40].

Figure 1d shows the FT-IR spectra of ZnSe and ZnSe:X that are 1% capped with MPA. It reveals that all of the samples were capped with an MPA agent. In comparison with MPA, the small peak at 2600 cm^{-1} that is assigned to the S-H vibration was diminished after the MPA was capped with ZnSe:X, which proposes the formation of the bond between metal and sulfur, including S-Zn, S-Ag, S-Cu, and S-Mg [58–61]. The broad absorption peaks in the range of $3410\text{--}3465\text{ cm}^{-1}$ that correspond to the -OH group indicate the existence of water absorbed onto the surfaces of the nanoparticles. The band at 2921 cm^{-1} is ascribed to the asymmetric stretching of C-H. The band at 2370 cm^{-1} is due to the C=O, and, at $1500\text{--}1650\text{ cm}^{-1}$, it is attributed to the C=O stretching mode that arises from the absorption of atmospheric CO_2 onto the surfaces of the nanoparticles [18,37]. Therefore, silver, copper, and magnesium are successfully doped into the ZnSe crystals.

Figure 2a shows that the diffraction patterns of the ZnSe:X that was 1% synthesized in an MPA capping agent possess zinc-blende crystal structures that display the cubic crystals at the (111), (220), and (311) planes, which correspond to 27.51° , 46.14° , and 53.85° , respectively (JCPDS Card No. 80-0021), and to 28° , 46° , and 54° , respectively. The X-ray diffraction patterns of the nanocrystalline ZnSe:Ag(1%), ZnSe:Cu(1%), and ZnSe:Mg(1%) powder samples show that the doped ZnSe:X was found to be of a cubical symmetry and that it is assigned to silver, copper, and magnesium, as confirmed from its standard JCPDS, No. 01-1167. [35,39,50,62]. No diffraction peaks from silver, copper, and magnesium impurities are detected in these samples. Therefore, it can be concluded that doping Ag^+ , Cu^{2+} , and Mg^{2+} into the host NPs does not generate a phase transformation of the crystal structure.

The TEM images of Ag^+ -, Cu^{2+} -, and Mg^{2+} -doped ZnSe nanoparticles are shown in Figure 2b. The images clearly show the formation of nanoparticles. The average sizes of the nanoparticles are 13.45 nm for ZnSe:Ag; 22.30 nm for ZnSe:Cu; and 24.10 nm for ZnSe:Mg. This can be explained by the fact that the ionic radii of Cu^{2+} (0.71 Å) and Mg^{2+} (0.72 Å) are closed to that of Zn^{2+} (0.74 Å), while the Ag^+ ion radius (1.14 Å) is larger than that of the Zn^{2+} (0.74 Å). Therefore, the ZnSe:Cu and ZnSe:Mg NPs have similar sizes, while the ZnSe:Ag size is much different from the other two NPs.

3.2. The Interaction of Nanoparticles with Amino Group (in lysine)

The amino group could react with the carboxylic (-COOH) of the MPA capped onto the ZnSe:X nanoparticles in the water solution by imide (-CONH) formation. Lysine is an essential amino acid that is involved in human metabolism, such as the urea cycle or the synthesis of polyamines. Thus, the interaction of NPs with an amino acid such as lysine is important for biosensor applications. Figure 3 shows the UV absorption of ZnSe:X-capped

MPA, with and without lysine. The absorption spectra of the ZnSe:X/MPA are unchanged after adding lysine, which suggests that lysine does not affect the size of the products.

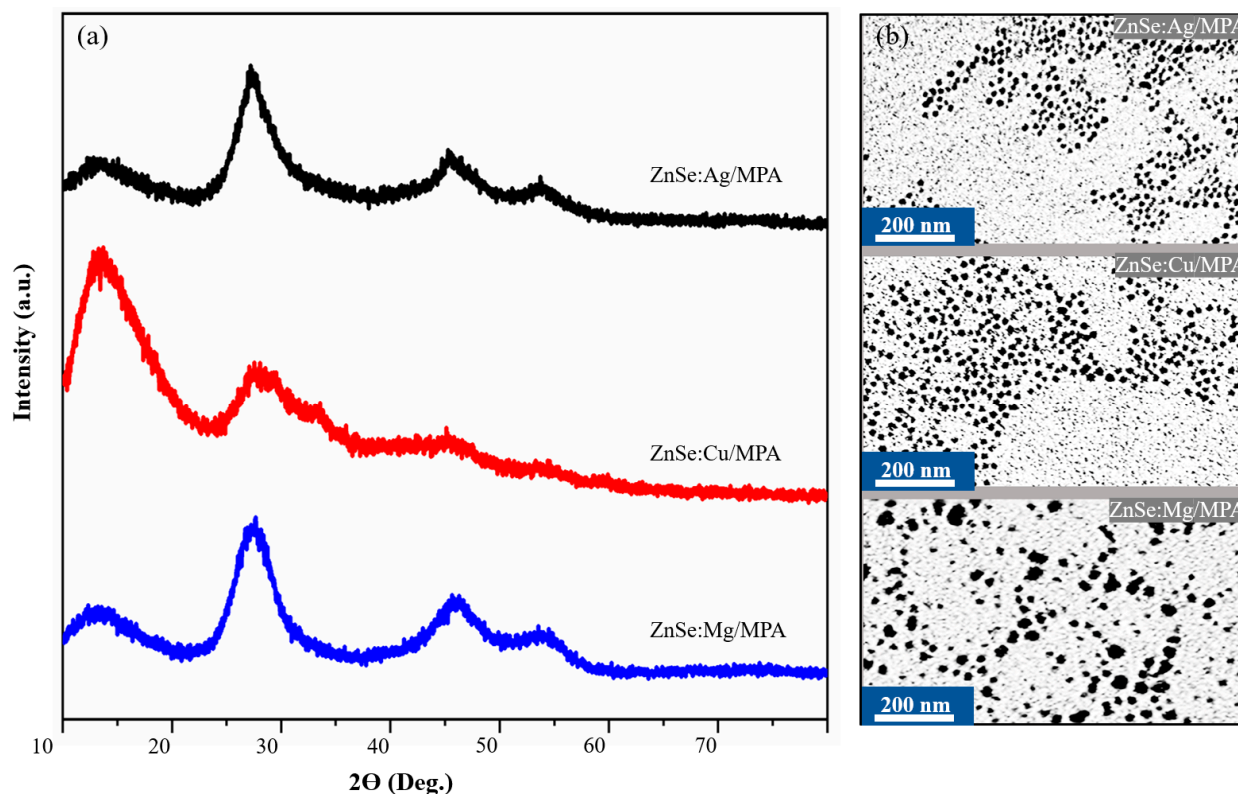


Figure 2. (a) The XRD patterns, and (b) TEM images of ZnSe:X (1%) at various dopants (Ag, Cu, and Mg).

However, the PL behavior depends on the addition of lysine (Figure 4). Obviously, the fluorescence intensity increases significantly with an increase in the lysine concentration. When the amount of amino acid is below 150 μL , the PL intensity does not change much (256.9–260.3–260.1). The volume of added lysine, especially, is raised to more than 200 μL , and the PL intensity is strongly increased. In addition, the maximum emission peak of ZnSe:Cu NPs is blue shifted, while the peaks of ZnSe:Ag and ZnSe:Mg are lightly redshifted when increasing the volume of lysine. This change confirms that the interaction between the ZnSe:X-capped MPA and the lysine has taken place. The electrostatic interaction between the amino group on the lysine and the carboxylic group on the MPA capping agent might help block the electron transfer, and then the HOMO–LUMO energy gaps of the ZnSe:X-capped MPA increases; consequently, the blue shift of the emission peak occurs. Moreover, because of this interaction, the number of activated electrons increases, which results in the increase in the number of excited electrons to the conducting band. Thus, the number of electrons of luminescence is raised as well. In other words, the lysine really affects the luminescent property of ZnSe:X NPs.

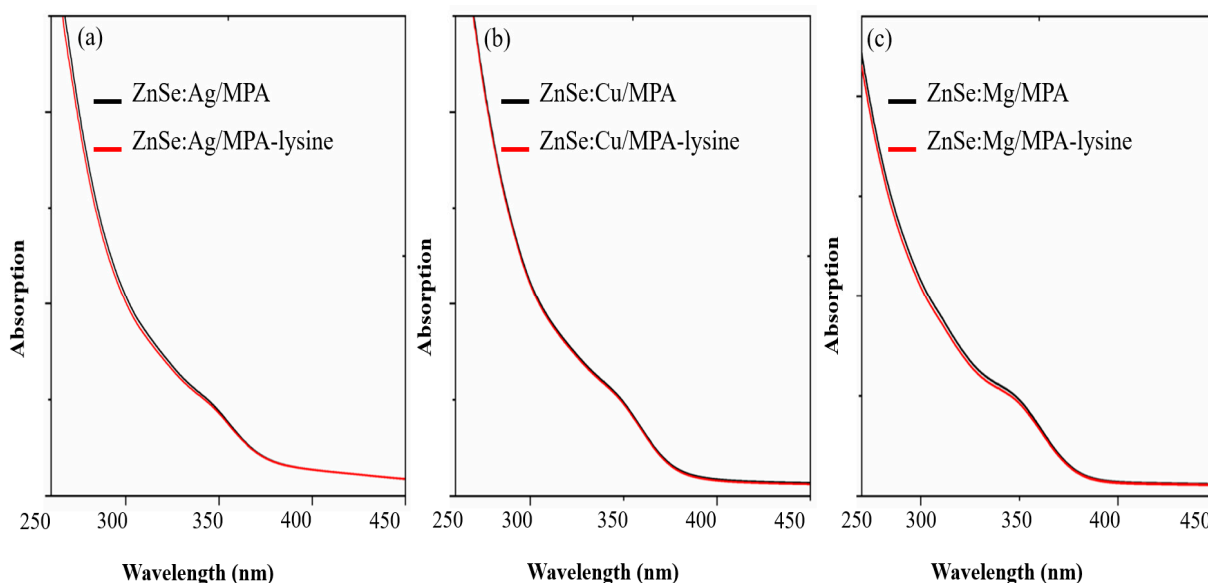


Figure 3. The UV spectra of ZnSe:X (1%) capped with MPA and lysine.

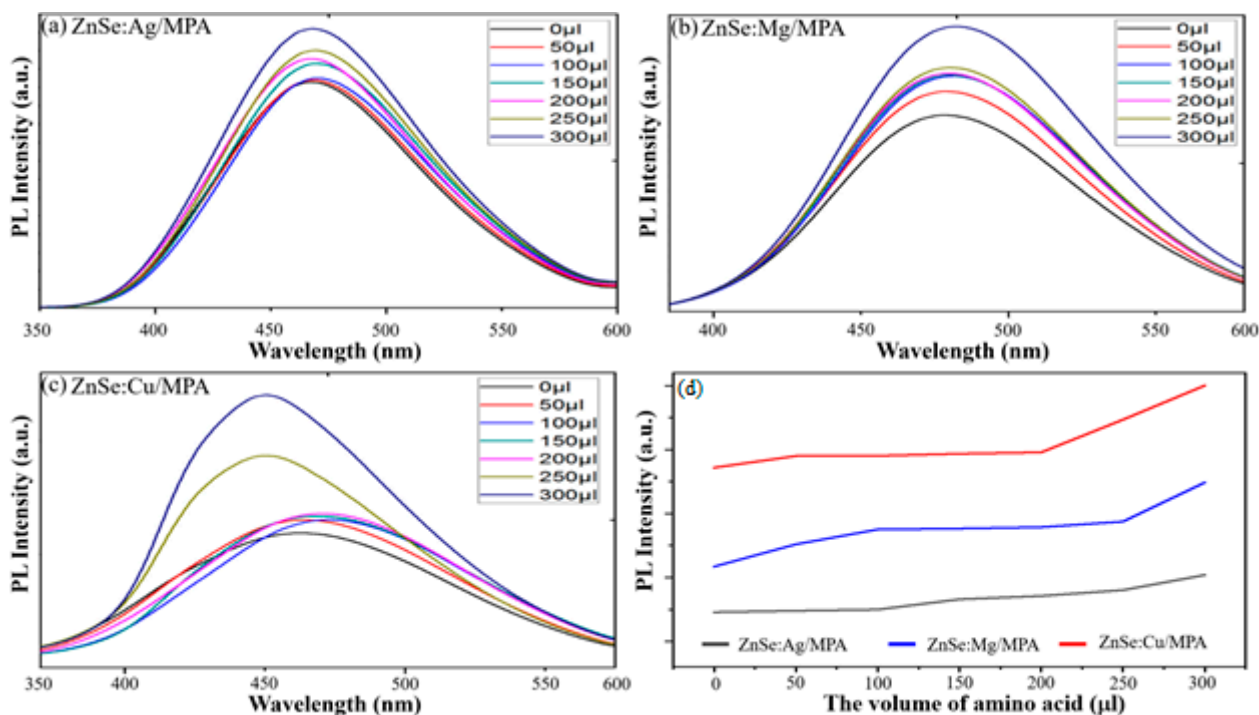


Figure 4. PL spectra of ZnSe:X-capped MPA combined with lysine: (a) ZnSe:Ag, (b) ZnSe:Cu, and (c) ZnSe:Mg; (d) the evaluation of the volume of lysine to the PL intensity at the maximum emission peak.

Figure 5 shows that each kind of NP produces a different sensitivity to lysine. Mg-doped NPs have the highest change in the PL intensity, which is 24.4% after adding lysine, whereas the change in the PL intensity is 13.6% and 10.5% in the cases of copper and silver, respectively. It is suggested that ZnSe:Mg could be a good candidates to apply in biosensors because of their high sensitivity to the amino group, which is present in all proteins of bacteria.

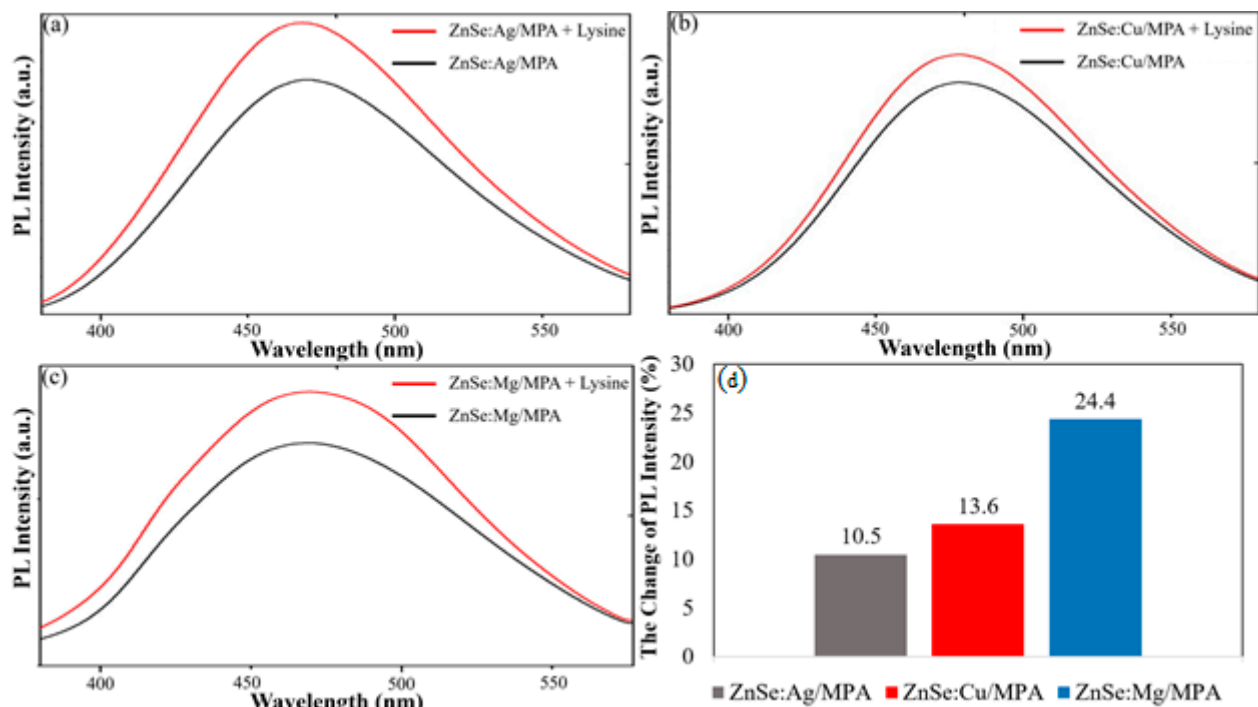


Figure 5. The PL intensity of ZnSe:X and ZnSe:X combined with lysine (0.3%): (a) ZnSe:Mg, (b) ZnSe:Cu, and (c) ZnSe:Ag; (d) the change in the PL intensity before and after adding lysine to ZnSe:X NPs.

3.3. Toxicity of ZnSe:X toward hMSCs

In order to establish ZnSe:X as a promising platform for biosensor purposes, a cellular viability study as a function of the concentration was performed with human mesenchymal stem cells (hMSCs). Our finding indicates that ZnSe:X decreased the hMSC viability in a dose-dependent manner, and that the toxicity of the ZnSe:X was highly impacted by the dopants (Figure 6a). The dramatic dose-dependent decrease in the hMSC viability was observed in ZnSe:Ag. With Mg, the toxicity of the NPs was ignored when the concentration was below 240 ppm. On the contrary, the transition metals (Ag and Cu) as dopants were relatively harmful to hMSCs. We also found that Ag-doped ZnSe was more toxic to hMSCs than Cu-doped ZnSe. A remarkable decrease, compared to the negative control sample, was detected in the hMSCs that were incubated with 60 ppm of ZnSe: Ag NPs ($p = 0.016$) and 120 ppm ZnSe:Cu NPs ($p = 0.004$). At 120 ppm, $79.80 \pm 1.03\%$ of the hMSCs were found to be visible in the ZnSe:Ag, while the viability of the cells that were cultured with ZnSe:Mg was $90.4 \pm 0.54\%$. More than one-half reductions in the hMSCs were observed in ZnSe:Ag at 320 ppm ($39.83 \pm 4.02\%$), while the hMSCs that were treated with ZnSe:Cu and ZnSe:Mg were $78.16 \pm 1.14\%$ and $85.00 \pm 1.95\%$, respectively. Furthermore, dual staining (AO/EB) was applied to verify the toxicity of ZnSe:X toward hMSCs (Figure 6b). No significant apoptotic was recorded in the negative control (0 ppm). The phenotypic characterization of the hMSCs that were cultured with ZnSe:Mg or ZnSe:Cu was identical to the negative control: a long fusiform shape. However, the hMSCs that were incubated with ZnSe:Ag displayed a flat polygonal shape with the significant change in the nucleus. Although the apoptosis sign was found in all the treated cells, the action was different. The late apoptosis sign (nucleus with orange-red color) was highly presented in the hMSCs that were treated with the silver dopant, while the other dopants displayed a few cells with early apoptosis features (bright-green nuclear). These observations prompted the further development of ZnSe:Mg or ZnSe:Cu as favorable materials for biolabeling purposes because of their relative non-cytotoxicity to hMSCs.

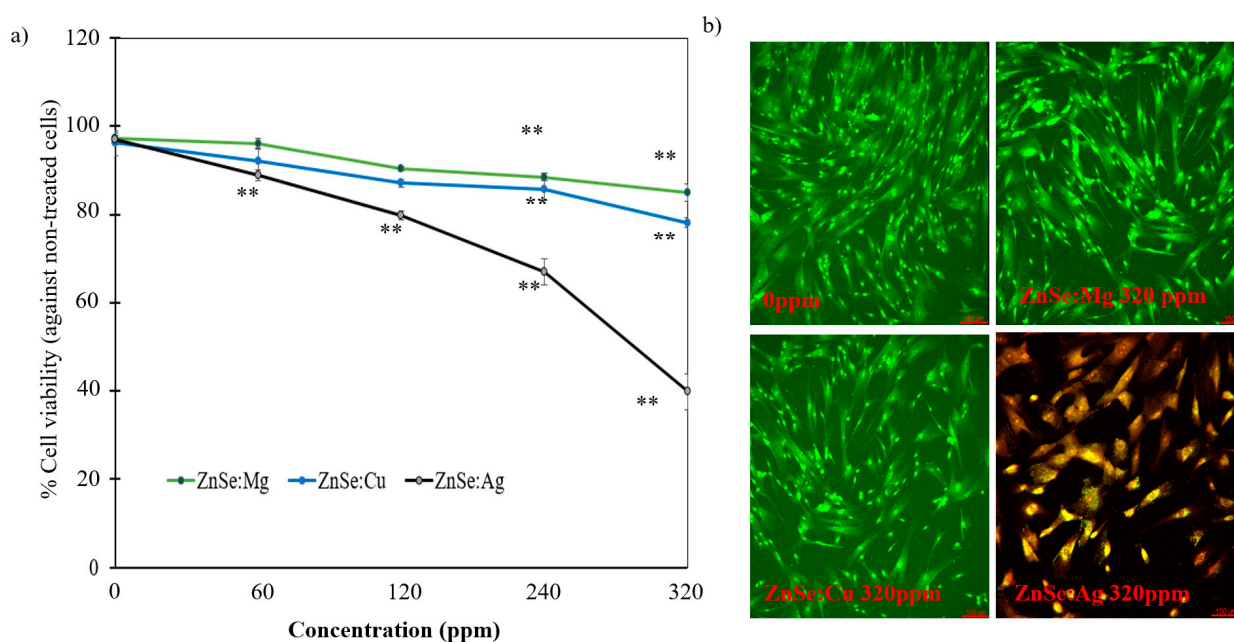


Figure 6. Cytotoxicity evaluation of ZnSe:X NC: (a) % of MSC cell viability after 48 h cultured with various concentrations of ZnSe:X. Data are presented as mean \pm SD of three independent replicated results. ** $p < 0.05$, as compared to negative control (DI water); (b) the confocal image of MSC cell by applied dual staining (AO/PI) after 48 h of treatment with different ZnSe:X at 320 ppm and 0 ppm. Scale bar: 150 μ m.

4. Conclusions

A facile and environmentally friendly aqueous synthesis of ZnSe:X (ZnSe:Ag, ZnSe:Cu, and ZnSe:Mg) NPs that uses mercaptopropionic acid (MPA) as a capping agent was introduced in this study. All of the resultant ZnSe:X NPs are well-dispersed in water and have a nano-sized structure. Their sizes are in the range of 10–30 nm, with cubic structural nanoparticles. All of the capping structure ZnSe:X NPs expose a blue photoluminescence band that is centered at around 440–480 nm. The PL intensity revealed the improvement in the emission through the changing of the dopants, from Ag to Cu to Mg. The photoluminescence quantum yields are in the following order: ZnSe:Ag (1%)-MPA (26%); ZnSe:Mg (1%)-MPA (32%); and ZnSe:Cu (1%)-MPA (40%). In addition, it was found that various concentrations of lysine can tune the PL intensity of ZnSe:X-capped MPA NPs, but do not affect their size. Through the change in the PL intensity after the addition of lysine, the Mg-doped ZnSe NPs demonstrated the highest sensitivity to lysine, compared to the transition-metal dopants. Along with the fluorescence behavior, the dopants induced a great impact on the cytotoxic profile of the ZnSe:X NPs. The viability of the hMSCs was over 80% when treated with ZnSe:Mg, even at the highest concentration of 320 ppm, while the transition-metal dopants induced relatively high toxicity to the cells, which provides critical information for the further study of Mg-doped ZnSe NPs for LEDs, sensors, and bacteria detectors.

Author Contributions: V.K.N., data curation, writing—original draft, formal analysis, visualization; D.K.P., data curation, writing—original draft, formal analysis, visualization; N.Q.T., conceptualization, writing—review and editing, formal analysis; L.H.D., writing—review and editing, formal analysis; N.H.N., writing—review and editing, formal analysis; T.V.N., writing—review and editing, formal analysis; T.B.L., conceptualization, writing—original draft, writing—review and editing, methodology, project administration. T.H.N., formal techniques to analyze. All authors have read and agreed to the published version of the manuscript.

Funding: This work was supported by the Vietnam National Foundation for Science and Technology Development (NAFOSTED) under the grant number: 104.01-2017.64.

Institutional Review Board Statement: Not applicable.

Informed Consent Statement: Not applicable.

Data Availability Statement: The data presented in this study are available upon request from the corresponding author.

Acknowledgments: We acknowledge the Vietnam National Foundation for Science and Technology Development (NAFOSTED) for the funding under the grant number: 104.01-2017.64. We also thank the Institute of Applied Materials Science and the Vietnam Academy of Science and Technology (VAST) for providing the necessary help during the work.

Conflicts of Interest: The authors declare no conflict of interest.

References

1. Constantine, C.A.; Gattás-Asfura, K.M.; Mello, S.V.; Crespo, G.; Rastogi, V.; Cheng, T.-C.; DeFrank, J.J.; Leblanc, R.M. Layer-by-layer biosensor assembly incorporating functionalized quantum dots. *Langmuir* **2003**, *19*, 9863–9867. [CrossRef]
2. Biju, V.; Muraleedharan, D.; Nakayama, K.-i.; Shinohara, Y.; Itoh, T.; Baba, Y.; Ishikawa, M. Quantum dot-insect neuropeptide conjugates for fluorescence imaging, transfection, and nucleus targeting of living cells. *Langmuir* **2007**, *23*, 10254–10261. [CrossRef] [PubMed]
3. Voura, E.B.; Jaiswal, J.K.; Mattoussi, H.; Simon, S.M. Tracking metastatic tumor cell extravasation with quantum dot nanocrystals and fluorescence emission-scanning microscopy. *Nat. Med.* **2004**, *10*, 993–998. [CrossRef] [PubMed]
4. Karakoti, A.S.; Shukla, R.; Shanker, R.; Singh, S. Surface of quantum dots for biological applications. *Adv. Colloid Interface Sci.* **2015**, *215*, 28–45. [CrossRef]
5. Luong, B.T.; Hyeong, E.; Ji, S.; Kim, N. Green synthesis of highly UV-orange emitting ZnSe/ZnS: Mn/ZnS core/shell/shell nanocrystals by a three-step single flask method. *RSC Adv.* **2012**, *2*, 12132–12135. [CrossRef]
6. Luong, B.T.; Hyeong, E.; Yoon, S.; Choi, J.; Kim, N. Facile synthesis of UV-white light emission ZnSe/ZnS: Mn core/(doped) shell nanocrystals in aqueous phase. *RSC Adv.* **2013**, *3*, 23395–23401. [CrossRef]
7. Draaisma, G.J.J.; Reardon, D.; Schenning, A.P.H.J.; Meskers, S.C.J.; Bastiaansen, C.W.M. Ligand exchange as a tool to improve quantum dot miscibility in polymer composite layers used as luminescent down-shifting layers for photovoltaic applications. *J. Mater. Chem. C* **2016**, *4*, 5747–5754. [CrossRef]
8. Zhang, B.; Wang, Y.; Hu, R.; Roy, I.; Yong, K.-T. Cadmium-free quantum dots for biophotonic imaging and sensing. In *Handbook of Photonics for Biomedical Engineering*; Ho, A.H.-P., Kim, D., Somekh, M.G., Eds.; Springer: Dordrecht, The Netherlands, 2017; pp. 841–870.
9. Mai, X.T.; Bui, D.T.; Bui, T.T.; Luong, B.T. Study of single-step synthesis of hyperbranched highly luminescence doped ZnSe:Mn, ZnSe:Mn/ZnS quantum dots and their interactions with acid amine. *J. Eng. Res.* **2018**, *7*, 27–32.
10. Xiong, S.; Huang, S.; Tang, A.; Teng, F. Synthesis and luminescence properties of water-dispersible ZnSe nanocrystals. *Mater. Lett.* **2007**, *61*, 5091–5094. [CrossRef]
11. Aboulaich, A.; Geszke, M.; Balan, L.; Ghanbaja, J.; Medjahdi, G.; Schneider, R. Water-based route to colloidal Mn-doped ZnSe and core/shell ZnSe/ZnS quantum dots. *Inorg. Chem.* **2010**, *49*, 10940–10948. [CrossRef]
12. Diaz-Diestra, D.; Beltran-Huarac, J.; Bracho-Rincon, D.P.; González-Feliciano, J.A.; González, C.I.; Weiner, B.R.; Morell, G. Biocompatible ZnS:Mn quantum dots for reactive oxygen generation and detection in aqueous media. *J. Nanoparticle Res.* **2015**, *17*, 461–473. [CrossRef] [PubMed]
13. Parani, S.; Tsolekile, N.; May, B.M.; Pandian, K.; Oluwafemi, O.S. Mn-doped ZnSe quantum dots as fluorimetric mercury sensor. In *Nonmagnetic and Magnetic Quantum Dots*. 2018. Available online: <https://www.intechopen.com/chapters/56882> (accessed on 10 March 2022).
14. Hu, Z.; Xu, S.; Xu, X.; Wang, Z.; Wang, Z.; Wang, C.; Cui, Y. Co-doping of Ag into Mn:ZnSe quantum dots: Giving optical filtering effect with improved monochromaticity. *Sci. Rep.* **2015**, *5*, 14817. [CrossRef] [PubMed]
15. Gao, M.; Kirstein, S.; Möhwald, H.; Rogach, A.L.; Kornowski, A.; Eychmüller, A.; Weller, H. Strongly photoluminescent CdTe nanocrystals by proper surface modification. *J. Phys. Chem. B* **1998**, *102*, 8360–8363. [CrossRef]
16. Wu, Y.A.; Warner, J.H. Shape and property control of Mn doped ZnSe quantum dots: From branched to spherical. *J. Mater. Chem.* **2012**, *22*, 417–424. [CrossRef]
17. Yu, J.H.; Kim, J.; Hyeon, T.; Yang, J. Facile synthesis of manganese (II)-doped ZnSe nanocrystals with controlled dimensionality. *J. Chem. Phys.* **2019**, *151*, 244701. [CrossRef]
18. Murase, N.; Gao, M. Preparation and photoluminescence of water-dispersible ZnSe nanocrystals. *Mater. Lett.* **2004**, *58*, 3898–3902. [CrossRef]
19. Dahl, J.A.; Maddux, B.L.S.; Hutchison, J.E. Toward greener nanosynthesis. *Chem. Rev.* **2007**, *107*, 2228–2269. [CrossRef]
20. Wei, Q.; Kang, S.-Z.; Mu, J. “Green” synthesis of starch capped CdS nanoparticles. *Colloid. Surf. A* **2004**, *247*, 125–127. [CrossRef]
21. Murphy, C.J. Sustainability as an emerging design criterion in nanoparticle synthesis and applications. *J. Mater. Chem.* **2008**, *18*, 2173–2176. [CrossRef]

22. Senthilkumar, K.; Thirunavukarasu, K.; Samikannu, K.; Balasubramanin, V. Low temperature method for synthesis of starch-capped ZnSe nanoparticles and its characterization studies. *J. Appl. Phys.* **2012**, *112*, 114331–153111. [[CrossRef](#)]
23. Pandey, V.; Tripathi, V.K.; Singh, K.K.; Bhatia, T.; Upadhyay, N.K.; Goyal, B.; Pandey, G.; Hwang, I.; Tandon, P. Nitrogen donor ligand for capping ZnS quantum dots: A quantum chemical and toxicological insight. *RSC Adv.* **2019**, *9*, 28510–28524. [[CrossRef](#)]
24. Winiarz, J.G.; Zhang, L.; Lal, M.; Friend, C.S.; Prasad, P.N. Photogeneration, charge transport, and photoconductivity of a novel PVK/CdS-nanocrystal polymer composite. *Chem. Phys.* **1999**, *245*, 417–428. [[CrossRef](#)]
25. Babu, R.; Zhang, J.; Beckman, E.J.; Virji, M.; Pasculle, W.A.; Wells, A.J.B. Antimicrobial activities of silver used as a polymerization catalyst for a wound-healing matrix. *Biomaterials* **2006**, *27*, 4304–4314. [[CrossRef](#)] [[PubMed](#)]
26. Ciobanu, C.S.; Massuyeau, F.; Constantin, L.V.; Predoi, D.J.N.R.L. Structural and physical properties of antibacterial Ag-doped nano-hydroxyapatite synthesized at 100 C. *Nanoscale Res. Lett.* **2011**, *6*, 613. [[CrossRef](#)]
27. Lok, C.-N.; Ho, C.-M.; Chen, R.; He, Q.-Y.; Yu, W.-Y.; Sun, H.; Tam, P.K.-H.; Chiu, J.-F.; Che, C.-M. Silver nanoparticles: Partial oxidation and antibacterial activities. *JBIC J. Biol. Inorg. Chem.* **2007**, *12*, 527–534. [[CrossRef](#)]
28. Zhang, X.T.; Ip, K.M.; Li, Q.; Hark, S.K. Photoluminescence of Ag-doped ZnSe nanowires synthesized by metalorganic chemical vapor deposition. *Appl. Phys. Lett.* **2005**, *86*, 203114. [[CrossRef](#)]
29. Wang, C.; Xu, S.; Shao, Y.; Wang, Z.; Xu, Q.; Cui, Y. Synthesis of Ag doped ZnInSe ternary quantum dots with tunable emission. *J. Mater. Chem. C* **2014**, *2*, 5111–5115. [[CrossRef](#)]
30. Xi, Y.; Bouanani, L.E.; Xu, Z.; Quevedo-Lopez, M.A.; Minary-Jolandan, M. Solution-based Ag-doped ZnSe thin films with tunable electrical and optical properties. *J. Mater. Chem. C* **2015**, *3*, 9781–9788. [[CrossRef](#)]
31. Sharma, M.; Sen, S.; Gupta, J.; Ghosh, M.; Pitale, S.; Gupta, V.; Gadkari, S.C. Tunable blue-green emission from ZnS(Ag) nanostructures grown by hydrothermal synthesis. *J. Mater. Res.* **2018**, *33*, 3963–3970. [[CrossRef](#)]
32. Muntaz Begum, S.; Rao, M.C.; Ravikumar, R.V.S.S.N. Cu²⁺ doped PVA passivated ZnSe nanoparticles-preparation, characterization and properties. *J. Inorg. Organomet. Polym. Mater.* **2013**, *23*, 350–356. [[CrossRef](#)]
33. Khafajeh, R.; Molaei, M.; Karimipour, M. Synthesis of ZnSe and ZnSe:Cu quantum dots by a room temperature photochemical (UV-assisted) approach using Na(2) SeO(3) as Se source and investigating optical properties. *Luminescence* **2017**, *32*, 581–587. [[CrossRef](#)] [[PubMed](#)]
34. Gong, F.; Sun, L.; Ruan, H.; Cai, H. Hydrothermal synthesis and photoluminescence properties of Cu-doped ZnSe quantum dots using glutathione as stabilizer. *Mater. Express* **2018**, *8*, 173–181. [[CrossRef](#)]
35. Wu, Y.; Chen, S.; Weng, Y.; Zhang, Y.; Wu, C.; Sun, L.; Zhang, S.; Yan, Q.; Guo, T.; Zhou, X. Facile synthesis and color conversion of Cu-doped ZnSe quantum dots in an aqueous solution. *J. Mater. Sci. Mater. Electron.* **2019**, *30*, 21406–21415. [[CrossRef](#)]
36. Khezripour, A.R.; Souri, D. PH-, microwave irradiation time-, and dopant content- sensitive photoluminescence of pure and Cu-doped ZnSe quantum dots fabricated by rapid microwave activated method. *Optik* **2019**, *183*, 294–301. [[CrossRef](#)]
37. Kumar, R.A.; Prasad, M.V.V.K.S.; Kiran Kumar, G.; Venkateswarlu, M.; Rajesh, C. Tuning of emission from copper-doped ZnSe quantum dots. *Phys. Scr.* **2019**, *94*, 115806. [[CrossRef](#)]
38. Bahador, A.R.; Molaei, M.; Karimipour, M. One-pot room temperature synthesizing Cu- and Mn-doped ZnSe nanocrystals by a rapid photochemical method. *Mod. Phys. Lett. B* **2016**, *30*, 1650227. [[CrossRef](#)]
39. Archana, J.; Navaneethan, M.; Prakash, T.; Ponnusamy, S.; Muthamizhchelvan, C.; Hayakawa, Y. Chemical synthesis and functional properties of magnesium doped ZnSe nanoparticles. *Mater. Lett.* **2013**, *100*, 54–57. [[CrossRef](#)]
40. Huy, B.T.; Seo, M.-H.; Phong, P.T.; Lim, J.-M.; Lee, Y.-I. Facile synthesis of highly luminescent Mg(II), Cu(I)-codoped CdS/ZnSe core/shell nanoparticles. *Chem. Eng. J.* **2014**, *236*, 75–81. [[CrossRef](#)]
41. Pradhan, N.; Goorskey, D.; Thessing, J.; Peng, X. An Alternative of CdSe nanocrystal emitters: Pure and tunable impurity emissions in ZnSe nanocrystals. *J. Am. Chem. Soc.* **2005**, *127*, 17586–17587. [[CrossRef](#)]
42. Shavel, A.; Gaponik, N.; Eychmüller, A. Efficient UV-blue photoluminescing thiol-stabilized water-soluble alloyed ZnSe(S) nanocrystals. *J. Phys. Chem. B* **2004**, *108*, 5905–5908. [[CrossRef](#)]
43. Fang, Z.; Wu, P.; Zhong, X.; Yang, Y.-J. Synthesis of highly luminescent Mn:ZnSe/ZnS nanocrystals in aqueous media. *Nanotechnology* **2010**, *21*, 305604. [[CrossRef](#)] [[PubMed](#)]
44. Wang, C.; Gao, X.; Ma, Q.; Su, X. Aqueous synthesis of mercaptopropionic acid capped Mn²⁺-doped ZnSe quantum dots. *J. Mater. Chem.* **2009**, *19*, 7016–7022. [[CrossRef](#)]
45. Lan, G.-Y.; Lin, Y.-W.; Huang, Y.-F.; Chang, H.-T. Photo-assisted synthesis of highly fluorescent ZnSe(S) quantum dots in aqueous solution. *J. Mater. Chem.* **2007**, *17*, 2661–2666. [[CrossRef](#)]
46. Norman, T.J.; Magana, D.; Wilson, T.; Burns, C.; Zhang, J.Z.; Cao, D.; Bridges, F. Optical and surface structural properties of Mn²⁺-Doped ZnSe nanoparticles. *J. Phys. Chem. B* **2003**, *107*, 6309–6317. [[CrossRef](#)]
47. Hill, N.A.; Whaley, K.B. A theoretical study of the influence of the surface on the electronic structure of CdSe nanoclusters. *J. Chem. Phys.* **1994**, *100*, 2831–2837. [[CrossRef](#)]
48. Underwood, D.F.; Kippeny, T.; Rosenthal, S.J. Ultrafast carrier dynamics in cdse nanocrystals determined by femtosecond fluorescence upconversion spectroscopy. *J. Phys. Chem. B* **2001**, *105*, 436–443. [[CrossRef](#)]
49. Becker, W.G.; Bard, A.J. Photoluminescence and photoinduced oxygen adsorption of colloidal zinc sulfide dispersions. *J. Phys. Chem.* **1983**, *87*, 4888–4893. [[CrossRef](#)]
50. Yadav, K.; Jaggi, N. Effect of Ag doping on structural and optical properties of ZnSe nanophosphors. *Mater. Sci. Semicon. Process.* **2015**, *30*, 376–380. [[CrossRef](#)]

51. Xu, S.; Wang, C.; Wang, Z.; Cui, Y. Theoretical and experimental investigation of stability and spectra of doped Ag:ZnSe nanocrystals. *J. Mol. Model.* **2014**, *20*, 2184. [[CrossRef](#)]
52. Cao, L.X.; Sun, D.K.; Lin, Y.X. Preparation and luminescence properties of core-shell ZnS: Cu/ZnS nano-particles. *Guang Pu Xue Yu Guang Pu Fen Xi* **2006**, *26*, 2000–2002.
53. Suyver, J.F.; van der Beek, T.; Wuister, S.F.; Kelly, J.J.; Meijerink, A. Luminescence of nanocrystalline ZnSe:Cu. *Appl. Phys. Lett.* **2001**, *79*, 4222–4224. [[CrossRef](#)]
54. Han, J.; Zhang, H.; Tang, Y.; Liu, Y.; Yao, X.; Yang, B. Role of redox reaction and electrostatics in transition-metal impurity-promoted photoluminescence evolution of water-soluble ZnSe nanocrystals. *J. Phys. Chem. C* **2009**, *113*, 7503–7510. [[CrossRef](#)]
55. Molaei, M.; Khezripour, A.R.; Karimipour, M. Synthesis of ZnSe nanocrystals (NCs) using a rapid microwave irradiation method and investigation of the effect of copper (Cu) doping on the optical properties. *Appl. Surf. Sci.* **2014**, *317*, 236–240. [[CrossRef](#)]
56. Rajesh, C.; Phadnis, C.V.; Sonawane, K.G.; Mahamuni, S. Synthesis and optical properties of copper-doped ZnSe quantum dots. *Phys. Scr.* **2014**, *90*, 015803. [[CrossRef](#)]
57. Han, J.; Zhang, H.; Sun, H.; Zhou, D.; Yang, B. Manipulating the growth of aqueous semiconductor nanocrystals through amine-promoted kinetic process. *Phys. Chem. Chem. Phys.* **2010**, *12*, 332–336. [[CrossRef](#)]
58. Zhang, B.-H.; Wu, F.-Y.; Wu, Y.-M.; Zhan, X.-S. Fluorescent method for the determination of sulfide anion with zns:mn quantum dots. *J. Fluoresc.* **2010**, *20*, 243–250. [[CrossRef](#)]
59. Guo, K.; Han, F.; Arslan, Z.; McComb, J.; Mao, X.; Zhang, R.; Sudarson, S.; Yu, H. Adsorption of Cs from water on surface-modified MCM-41 mesosilicate. *Water Air Soil Pollut.* **2015**, *226*, 288. [[CrossRef](#)]
60. Liu, L.; Peng, M.; Xia, H.; Li, N. Key factors in the stability of doped ZnSe:Mn@MPA semiconductor nanocrystals. *Chem. Phys. Lett.* **2019**, *730*, 544–550. [[CrossRef](#)]
61. Huang, F.; Huang, T.; Wu, X.; Pang, W. Synthesis and characterization of ZnSe: Ag/SiO₂ nanoparticles. *E3S Web Conf.* **2021**, *261*, 02063. [[CrossRef](#)]
62. Zheng, Y.; Yang, Z.; Ying, J.Y. Aqueous synthesis of glutathione-capped ZnSe and Zn_{1-x}Cd_xSe alloyed quantum dots. *Adv. Mater.* **2007**, *19*, 1475–1479. [[CrossRef](#)]